ACS APPLIED MATERIALS & INTERFACES

Research Article

Cite This: ACS Appl. Mater. Interfaces 2019, 11, 36607−36615

www.acsami.org

Thermodynamic Assessment of Coating Materials for Solid-State Li, Na, and K Batteries

Seungho Yu,*[,†,⊥] Haesun Park,[†] and Donald J. Siegel*[,†,‡,§,∥]

[†]Mechanical Engineering Department, [‡]Materials Science & Engineering, [§]Applied Physics Program, and [∥]University of Michigan Energy Institute, University of Michigan, Ann Arbor, Michigan 48109-2125, United States

[⊥]Center for Energy Storage Research, Korea Institute of Science and Technology (KIST), 5, Hwarang-ro 14-gil, Seongbuk-gu, Seoul 02792, Republic of Korea

Supporting Information

ABSTRACT: The development of all-solid-state batteries (ASSBs) presents a pathway to enhance the energy density and safety of conventional Li-ion batteries that use liquid electrolytes. However, one of the more promising categories of solid electrolytes (SEs), sulfides, are generally unstable in contact with common electrode materials, resulting in SE decomposition and high interfacial resistance. Recent studies have indicated that the application of coatings can, in some cases, stabilize the electrode/SE interface, reducing the likelihood for harmful interfacial reactions. Here, stable coatings for Li, Na, and K ASSBs are identified. In total, the stability windows for 1112 ternary alkali-metal-based compounds were assessed, including fluorides, chlorides, oxides, sulfides, phosphides, and nitrides. In general, the fluorides and chlorides exhibit the highest oxidative stability, suggesting that they are good choices for stabilizing SE/cathode interfaces. In contrast, sulfides, phosphides, and nitrides exhibit much lower oxidative stabilities, with many of these materials predicted to decompose above 2 V. At the anode/SE interface, nitrides and oxides are predicted to be the most effective coatings, as they are generally the most stable against reductive decomposition. As expected, sulfides and phosphides are the least stable class of materials under reducing conditions. Overall, oxides appear to be the most versatile class of coating materials: several oxides are predicted to exhibit stability windows ranging from 0 to 3 V with respect to Li/Li^+, Na/Na^+, or K/K^+. Examples of promising oxides for stabilizing the SE/anode interface include Li_5AlO_4, Li_4SiO_4, $NaAlO_2$, Na_3PO_4, $KAlO_2$, and K_3PO_4. Similarly, promising compounds for stabilizing the SE/cathode interface include $NaPO_3$ and KPO_3. Finally, the possibility for kinetic stabilization suggests that additional ternary oxides (e.g., based on Ga, Nb, Sb, and Ta) may be viable coatings at the SE/cathode interface.

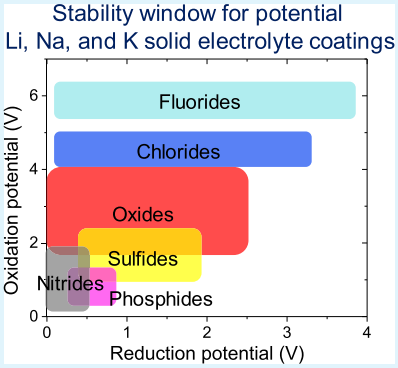

KEYWORDS: *energy storage, batteries, solid electrolytes, high-throughput screening, coating materials*

INTRODUCTION

Batteries with high energy density and enhanced safety are desired for emerging applications such as electric vehicles.[1,2] A promising pathway to enhance the performance of batteries is through the development of solid electrolytes (SEs).[3,4] In principle, a suitable SE would allow substituting the conventional graphite-based anode used in Li-ion batteries with metallic Li, increasing the energy density of the anode. On the cathode side, an SE could also enable the use of high-capacity cathodes such as Li−S and Li−air.[5,6] Finally, SEs can also improve battery safety by replacing flammable organic liquid electrolytes with a more stable solid.[7]

Various SEs have been developed for all solid-state batteries (ASSBs).[8−10] Among Li-ion conducting SEs, sulfides have shown highest ionic conductivities.[8,11,12] For example, the conductivity of $Li_{10}GeP_2S_{12}$ has been reported at 12 mS/cm, comparable to that of liquid electrolytes used in conventional Li-ion batteries.[13] However, interfacial decomposition of sulfide SEs occurs upon contact with Li metal electrodes, resulting in undesirable increases in interfacial resistance.[14−16] Recent first-principles computational studies have provided an explanation for this behavior by predicting that the Li sulfide SEs have relatively narrow electrochemical stability windows.[15−18] Recently, similar studies have been performed on the stability windows of Na SEs.[19,20] Na sulfide SEs exhibited narrow windows of 1.4−2.5, 1.8−1.9, and 1.4−2.2 V for Na_3PS_4, Na_3SbS_4, and $Na_{10}SnP_2S_{12}$, respectively,[19] indicating that decomposition of SEs will occur upon contact with electrodes that operate at voltages outside of these relatively narrow limits.

Protective coatings between the SE and the electrode could prevent or slow these decomposition reactions.[15,21] A previous computational study showed that several Li binary compounds and five Li ternary compounds could be used as stable coating materials for Li SEs.[19] Experimental studies have also examined several Li-based coatings such as $LiAlO_2$,[22] Li_3BO_3,[23]

Received: June 23, 2019
Accepted: September 16, 2019
Published: September 16, 2019

DOI: 10.1021/acsami.9b11001
ACS Appl. Mater. Interfaces 2019, 11, 36607−36615

Li_2SiO_3,[24] and Li_3PO_4.[25] Recently, high-throughput screening was performed to find stable coatings for Li and Na ASSBs.[19,20,26] For Li SEs, LiH_2PO_4, $LiTi_2(PO_4)_3$, and $LiPO_3$ were identified as promising cathode-coating materials.[28] Several oxides were also found to be stable coating materials for Na SEs.[19] Recent studies that employ electrode coating materials have reported coating thicknesses ranging from approximately 5−50 nm.[21,27,28] These films are much thinner than that envisioned for a commercially viable SE, whose target thickness has been estimated to be on the order of tens of microns.[29]

Building on these earlier studies, the present work screens more than 1300 SE/electrode interfacial coatings for use in Li, Na, and K ASSBs. A wide composition space of binary and ternary compounds was examined, including fluorides, chlorides, oxides, sulfides, phosphides, and nitrides. Importantly, an assessment of coating materials for K ASSBs is reported for the first time. Trends in the stability windows among the different classes of coatings are discussed, and promising compositions are identified. In general, the fluorides and chlorides exhibit the highest oxidative stability, suggesting that they are good choices for stabilizing SE/cathode interfaces. In contrast, sulfides, phosphides, and nitrides exhibit much lower oxidative stabilities, with many of these materials predicted to decompose above 2 V. For the anode/SE interface, nitrides and oxides are predicted to be the most effective coatings as they are generally the most stable against reductive decomposition. As expected, the sulfides and phosphides are the least stable class of materials under reducing conditions. Overall, the oxides are predicted to be the most versatile class of coating materials: several oxides are predicted to exhibit stability windows ranging from 0 to 3 V with respect to Li/Li^+, Na/Na^+, or K/K^+. Examples of promising oxides for stabilizing the SE/anode interface include Li_5AlO_4, Li_4SiO_4, $NaAlO_2$, Na_3PO_4, $KAlO_2$, and K_3PO_4. Similarly, promising compounds for stabilizing the SE/cathode interface include $NaPO_3$ and KPO_3. In addition, ternary oxides (based, e.g., on Ga, Nb, Sb, and Ta) may be viable coatings at the SE/cathode interface based on the possibility for kinetic stabilization.

METHODS

The total energies of all materials examined in this study were obtained from the Materials Project (MP) database.[30] These energies were derived from density functional theory calculations performed using a plane wave basis set, the projector augmented wave method,[31] and the generalized gradient approximation in the Perdew−Burke−Ernzerhof formulation,[32] as implemented in the Vienna Ab initio Simulation Package.[33] An energy correction was applied for anions, transition metals, and gas/liquid phases in the MP, as previously described.[34−36]

The electrochemical stability of the coating materials was determined using the grand potential phase diagram as a function of chemical potential μ_A (A = Li, Na, and K), which is given by,

$$\mu_A(\varphi) = \mu_{A,0} - e\varphi \quad (1)$$

where $\mu_{A,0}$ is the chemical potential of element A (A = Li, Na, and K), e is the elementary charge, and φ is the potential referenced to the metal anode. (This approach could be extended to multivalent battery chemistries such as Mg and Al simply by screening for compounds containing those elements.) The Pymatgen code was used to generate the grand potential phase diagram,[34] which presents the most stable phase(s) in a given composition space as a function of chemical potential μ_A. A description of the methods used to construct grand potential phase diagrams is reported elsewhere.[15,16,37]

It should be noted that the analysis presented here applies to stability as a function of the electrochemical potential relative to that of the (Li, Na, or K) metal anode. In this sense, it captures the potential-dependent stability at both the negative and positive electrodes. (The coating will experience different potentials at interfaces with the two electrodes, and these different conditions could induce decomposition.) What this approach does not capture is chemical reactivity with cathodes that contain elements beyond those present in the coating. For example, a Li−Al−O-based coating in contact with a Li−Co−O-based cathode could react to form a quaternary (Li−Al−Co−O) phase. Because of the many possible cathode materials, and our desire to maintain a "cathode agnostic" approach, chemical stability[16] with the cathode is not examined in the present study. Of course, the present analysis of electrochemical stability can be used as an initial filter to down-select suitable coating materials that can be subsequently examined with regard to their chemical stability (e.g., using the MP) once a specific cathode composition is specified.

As a first step, 662 A−X (A = Li, Na, and K) binary coating materials were collected from the MP database. Ternary compounds were also considered; because of the large number of possible ternaries, these materials were limited to fluorides, chlorides, oxides, sulfides, nitrides, and phosphides (A−M−X, X = F, Cl, O, S, N, and P). Initially, a total of 7207 ternary compounds were collected. Compounds including heavy elements (above row 7) were subsequently excluded. Next, the stability of the remaining compounds was assessed at 0 K using the convex hull method. Unstable compounds (i.e., all compounds above the convex hull) were excluded. A total of 220 binary compounds and 1112 ternary compounds satisfied this stability criterion and underwent further evaluation. In general, materials that are stable at 0 K (which lie on the convex hull) are considered "safe bets" to be realized/synthesized at room temperature (which adds only ∼26 meV/atom of thermal energy). Furthermore, compounds that are less than ∼50 meV/atom above the hull are also considered as plausible to be stabilized at elevated temperatures because of entropic contributions.[38] Because the present study only considers materials on the hull at 0 K, our analysis could be described as conservative. A more speculative approach comprising a larger group of candidate materials could be implemented by including metastable materials that were up to ∼25 meV above the hull.

Next, the electrochemical stability window of these 1332 compounds was obtained using the grand potential phase diagram. The stability window is defined as the range of potentials (eq 1) for which a given compound does not decompose. For coating materials between the anode and SE, the limit of this range, that is, the reduction potential, should ideally be negative with respect to the metal's equilibrium redox potential (defined as 0 V) to prevent decomposition when in contact with the anode metals. Nevertheless, sluggish kinetics may limit the decomposition reaction, even when the reduction potential of the coating material is more positive than 0 V. This phenomenon is referred to as "kinetic stabilization"; kinetic stabilization occurs when a material that is thermodynamically unstable under the given conditions does not react (or decompose) because of sluggish kinetics. Kinetic stabilization underlies the formation of the solid electrolyte interphase (SEI) in conventional (liquid-based) lithium-ion batteries.[7] By analogy with SEI formation, we have assumed that the sluggish kinetics may similarly stabilize the coating materials that do not possess a large driving force for reaction with a metal anode. A limited driving force is defined here as a decomposition voltage that is within +0.3 V of the standard potential for a given anode. This value was selected based on our prior study of Li_3BO_3 coatings,[39] which observed that Li_3BO_3 is unreactive with a Li metal anode—presumably because of slow kinetics—even though the associated reduction potential is +0.27 V.[39] Therefore, to allow for the possibility of kinetic stabilization, compounds with reduction potentials as high as +0.3 V were included. In addition, coating materials with a stability window narrower than 1.0 V were excluded.

For coatings envisioned for use between a cathode and the SE, compounds that exhibit oxidative stability to at least 4.0 V were

DOI: 10.1021/acsami.9b11001
ACS Appl. Mater. Interfaces 2019, 11, 36607−36615

selected; in addition, materials having a stability window narrower than 2.0 V were excluded. The ionic conductivity of the prospective coating materials was not assessed (and would be impractical to attempt, given the large number of materials examined). Because these systems are envisioned as thin coatings, a high ionic conductivity is not strictly required. For example, assuming a moderate area-specific resistance of the coating of 5 Ω cm^2, then a 10 nm (1 μm) coating would require a low conductivity of only 2 × 10^{-7} S/cm (2 × 10^{-5} S/cm).[40] These values are below the limit for superionic behavior.

RESULTS AND DISCUSSION

The stability window of 220 binary compounds was evaluated using the grand potential phase diagram. On the basis of the criteria described in the Methods section, 29 binary compounds were identified as prospective coating materials. Figure 1 shows the stability window of the 29 promising binary

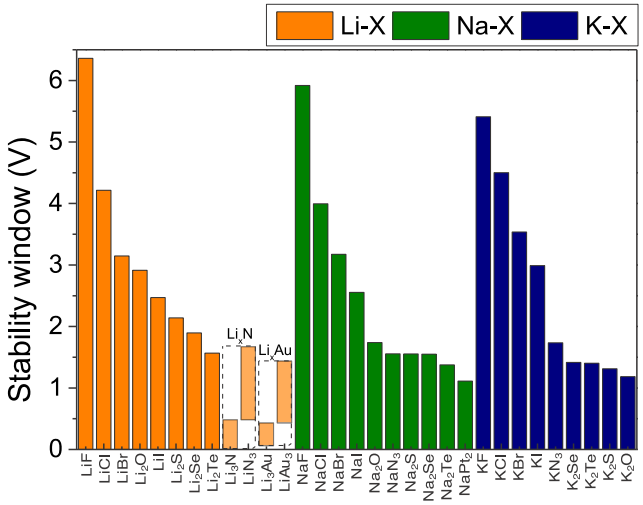

Figure 1. Predicted stability window of Li, Na, and K-based binary coating materials. The corresponding reduction and oxidation potentials are listed in Table S1.

compounds. The reduction and oxidation potentials calculated for the binaries are listed in Table S1. All binary compounds showed reduction potentials of approximately 0 V with respect to their alkaline metal and are therefore expected to be stable in contact with anodes comprising these metals.

Regarding oxidative stability, the halides (AX, X = F, Cl, Br, and I) were generally observed to possess the best performance. The halides also exhibited the widest stability windows, with the fluorides having the widest windows of 6.4, 5.9, and 5.4 V for LiF, NaF, and KF, respectively. The behavior of the fluorides was followed closely by the chlorides, with windows of 4.2, 4.0, and 4.5 V for LiCl, NaCl, and KCl, respectively. The chalcogenides (A_2X, X = O, S, Se, and Te) are predicted to be slightly less resistant to oxidation, with slightly lower voltages ranging from 1.2 to 2.9 V for the onset of oxidative decomposition. Finally, a few other binary coatings were predicted to be promising. For Li-ion batteries, Li_3N and Li_3Au are stable with respect to reduction against the Li metal anode (light orange bars shown in Figure 1). These two compounds are predicted to oxidize at a relatively low potential of ∼0.45 V, transforming into LiN_3 and $LiAu_3$, which are in turn stable against oxidation for potentials up to 1.67 and 1.44 V, respectively. Likewise, for sodium- and potassium-based cells, NaN_3, $NaPt_2$, and KN_3 are stable to 0 V and are stable against oxidation for voltages up to 1.56, 1.11, and 1.74 V, respectively.

Figure 2 illustrates the predicted reduction (*x*-axis) and oxidation (*y*-axis) potentials for 1112 ternary compounds. Figure 2a−c summarizes the data for 316 Li−M−X, 360 Na−M−X, and 436 K−M−X ternary compounds, respectively. In addition, the points shown in Figure 2 are colored based on the anion (X): light blue, blue, red, yellow, pink, and green indicate fluoride, chloride, oxide, sulfide, phosphide, and nitride, respectively. The approximate stable voltage windows for the different classes of ternary compounds are shown in Figure 2d.

Generally, fluorides (light blue data points) have the highest oxidation potentials, approximately 6 V, of the compounds examined. These high oxidation potentials suggest that they may be appropriate coatings between the cathode and SE. The chlorides also have high oxidation potentials of approximately 4 V. Regarding reduction potentials, the fluorides and chlorides exhibit a wide range of values spanning from 0 to 4 V. Fluorides and chlorides with reduction potentials of 0 V could be used as coating materials between the anode and SE. Compared to the behavior of the fluorides and chlorides, the reduction and oxidation potentials of the oxides fall within a wider range of values. Nevertheless, some oxides show good oxidative and/or reductive stability.

The sulfides, phosphides, and nitrides generally exhibit low oxidation potentials compared to those of fluorides, chlorides, and oxides. The average oxidation potentials of sulfides, phosphides, and nitrides were approximately 2, 1, and 1 V, respectively, which are inappropriate for coating materials on the cathode side of the SE. The reduction potential of the sulfides and phosphides were also greater than 0 V, suggesting that they are also not suitable choices for coating materials at the anode side of the SE. In contrast, several nitrides are stable against reduction to 0 V, indicating their potential use as coating materials between the anode and SE. This is in good agreement with earlier computational work that showed Li ternary nitrides are promising coating materials.[41]

Figure 3 shows the stability window of the most promising Li ternary coating materials for the (a) anode and (b) cathode side of the SE. As shown in Figure 2a, oxides and nitrides are the most stable at the anode side of the SE. No ternary Li fluorides, chlorides, sulfides, or phosphides were observed having reduction potentials less than 0.3 V. The most promising ternary Li oxides include $LiYO_2$, $Li_6Hf_2O_7$, $Li_6Zr_2O_7$, Li_5AlO_4, Li_2HfO_3, Li_4TiO_4, $LiAlO_2$, Li_8SiO_6, Li_4SiO_4, and Li_3BO_3. These compounds have low reduction potentials and wide stability windows of approximately 3 V. The Li ternary nitrides, Li_7VN_4, Li_2HfN_2, Li_2ZrN_2, Li_6CrN_4, Li_6MoN_4, Li_6WN_4, Li_5ReN_4, Li_4TaN_3, $LiTa_3N_4$, and $LiSi_2N_3$, also exhibit low reduction potentials. However, compared to the oxides, the nitrides have narrower stability windows of approximately 1 V. The reduction and oxidation potentials of all compounds shown in Figure 3a are summarized in Table S2.

Figure 3b shows the stability windows for the most promising fluorides, chlorides, and oxides for use as potential coatings at the interface between the cathode and SE. These compounds exhibited wide stability windows of at least 2 V, with oxidation potentials > 4 V. The most promising Li ternary fluorides include $LiYF_4$, Li_2BeF_4, Li_3AlF_6, Li_4ZrF_8, $LiTaF_6$, Li_2TiF_6, and $LiBF_4$. In the case of Li ternary chlorides and oxides, the most promising materials include Li_2MgCl_4, $LiAlCl_4$, Li_2MnCl_4, Li_2CdCl_4, Li_3PO_4, $LiAl_5O_8$, Li_2CO_3,

DOI: 10.1021/acsami.9b11001
ACS Appl. Mater. Interfaces 2019, 11, 36607−36615

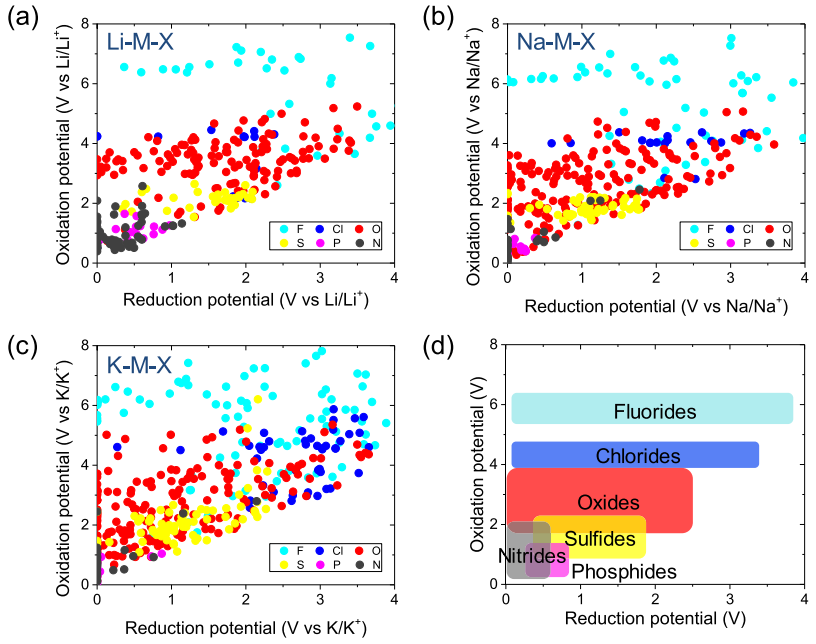

Figure 2. Reduction and oxidation potentials of ternary (a) Li−M−X, (b) Na−M−X, and (c) K−M−X compounds. Each point is colored based on the compound's anion (X): fluoride (light blue), chloride (blue), oxide (red), sulfide (yellow), phosphide (pink), and nitride (green). (d) Approximate reduction and oxidation potentials of the ternary compounds according to their anionic component.

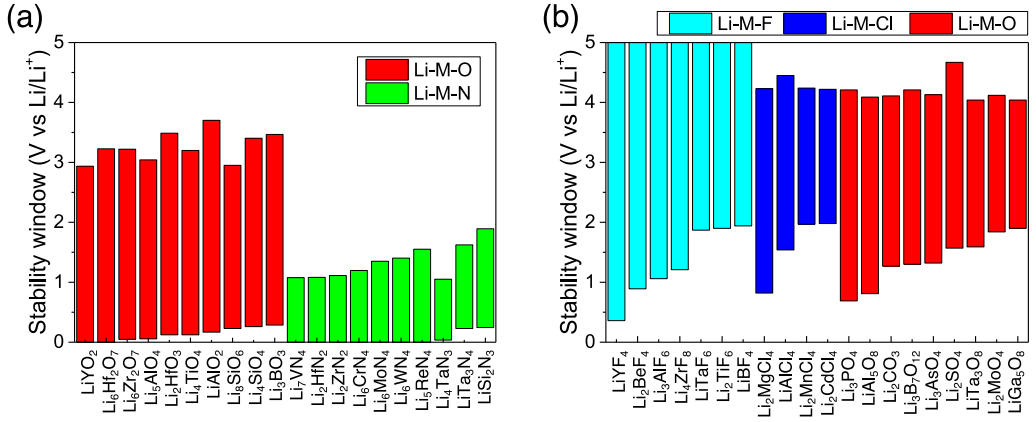

Figure 3. Stability windows of the most promising Li−M−X ternary coating materials for use at the (a) anode or (b) cathode. The reduction and oxidation potentials of these compounds are listed in Table 1. Anode materials were selected based on having a reductive stability of 0.3 V or less and a window of at least 1 V. Cathode materials have oxidative stabilities exceeding 4 V and a window of at least 2 V.

$Li_3B_7O_{12}$, Li_3AsO_4, Li_2SO_4, $LiTa_3O_8$, Li_2MoO_4, and $LiGa_5O_8$. As shown in Figure 2, none of the examined sulfides, phosphides, or nitrides were predicted to be suitable coatings for the interface between the cathode and SE.

A handful of other coating materials show promise upon relaxing the requirement for a minimum oxidative stability from 4 to 3.5 V and allowing a window of width smaller than 2 V. For example, $LiGaO_2$, Li_4GeO_4, $LiNbO_3$, Li_2SnO_3, Li_3SbO_4, and Li_3TaO_4 have oxidation potentials of 3.81, 3.39, 3.88, 3.53, 3.57, and 3.60 V with reduction potentials of 1.05, 1.02, 1.74, 1.36, 1.64, and 0.54 V, respectively, as shown in Table 1. These materials may be of use as coatings on the cathode side of the SE.

Figure 4 shows the phase diagrams for three ternary Li oxide systems, Li−M−O, based on Al, Si, and B, respectively. Several compositions within these systems are relatively stable in contact with Li metal and have a stability window greater than 3 V. Hence, these coatings could be used at both interfaces of SEs (in contact with both the anode and cathode). In the Li−Al−O system, three phases are noteworthy: Li_5AlO_4, $LiAlO_2$, and $LiAl_5O_8$. Of these, $LiAlO_2$ exhibited the widest stability window, ranging from 0.17 to 3.70 V, while Li_5AlO_4 is predicted to be the most stable against reduction. Stable ternaries in the Li−Si−O system include Li_8SiO_6, Li_4SiO_4, Li_2SiO_3, and $Li_2Si_2O_5$. Of these phases, both Li_4SiO_4 and Li_8SiO_6 are stable to relatively low voltages of 0.26 and 0.23 V. The former compound also has relatively high oxidation potential of 3.41 V. Several phases are stable in the Li−B−O phase diagram, including Li_3BO_3, $Li_6B_4O_9$, $LiBO_2$, $Li_2B_4O_7$, $Li_3B_7O_{12}$, and $Li_3B_{11}O_{18}$. Out of these possibilities, Li_3BO_3 is the most promising coating material because of its wide stability window of 0.28−3.47 V.

Figure 4 also shows that reductive stability in the Li−Al−O, Li−Si−O, and Li−B−O systems increases with lithium content. For example, the most Li-rich phases, Li_5AlO_4, Li_8SiO_6, and Li_3BO_3, have the lowest reduction potentials,

DOI: 10.1021/acsami.9b11001
ACS Appl. Mater. Interfaces 2019, 11, 36607−36615

Table 1. Stability Windows (in V) for Several Li-, Na-, and K-Based Ternary Oxides Exhibiting Oxidative Stabilities Generally below 4 V[a]

M	Li−M−O		Na−M−O		K−M−O	
B	Li_3BO_3	0.28−3.47	Na_3BO_3	0.00−2.67	KBO_2	0.00−3.17
Al	$LiAlO_2$	0.17−3.70	$NaAlO_2$	0.00−3.19	$KAlO_2$	0.00−3.04
Si	Li_4SiO_4	0.26−3.41	Na_2SiO_3	0.00−3.15	K_2SiO_3	0.00−3.00
P	Li_3PO_4	0.69−4.21	Na_3PO_4	0.00−3.27	K_3PO_4	0.00−3.36
	$LiPO_3$	2.48−4.99	$NaPO_3$	1.91−4.69	KPO_3	1.55−4.94
Ti	Li_4TiO_4	0.12−3.20	Na_4TiO_4	0.00−2.68	K_4TiO_4	0.00−2.12
Ga	$LiGaO_2$	1.05−3.81	$NaGaO_2$	0.23−3.24	$KGaO_2$	0.14−3.12
Ge	Li_4GeO_4	1.02−3.39	Na_4GeO_4	0.00−2.67	K_4GeO_4	0.00−2.25
Zr	Li_2ZrO_3	0.34−3.41	Na_2ZrO_3	0.00−2.92	K_2ZrO_3	0.00−2.37
Nb	$LiNbO_3$	1.74−3.88	$NaNbO_3$	0.88−3.60	$KNbO_3$	0.00−3.36
Sn	Li_2SnO_3	1.36−3.53	Na_2SnO_3	0.42−3.08	K_2SnO_3	0.73−2.45
Sb	Li_3SbO_4	1.64−3.57	Na_3SbO_4	0.66−2.90	K_3SbO_4	0.72−2.25
	$LiSbO_3$	2.23−4.14	$NaSbO_3$	1.46−3.99	$KSbO_3$	1.26−3.77
Ta	Li_3TaO_4	0.54−3.60	$NaTaO_3$	0.02−3.61	$KTaO_3$	0.00−3.60

[a]Despite their lower oxidative stability, these materials could be viable coating materials for the cathode/SE interface if slow kinetics inhibits their decomposition.

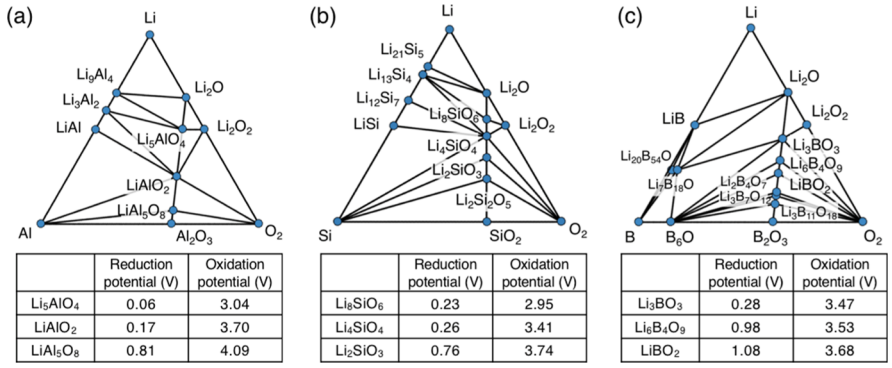

	Reduction potential (V)	Oxidation potential (V)
Li_5AlO_4	0.06	3.04
$LiAlO_2$	0.17	3.70
$LiAl_5O_8$	0.81	4.09

	Reduction potential (V)	Oxidation potential (V)
Li_8SiO_6	0.23	2.95
Li_4SiO_4	0.26	3.41
Li_2SiO_3	0.76	3.74

	Reduction potential (V)	Oxidation potential (V)
Li_3BO_3	0.28	3.47
$Li_6B_4O_9$	0.98	3.53
$LiBO_2$	1.08	3.68

Figure 4. Phase diagrams for the (a) Li−Al−O, (b) Li−Si−O, and (c) Li−B−O systems. The stability windows of promising coating materials from each composition space are listed below each phase diagram. (All calculations are performed at 0 K.)

while the most Li-deficient ones, $LiAl_5O_8$, Li_2SiO_3, and $LiBO_2$, are the least stable against reduction (decomposing below 0.81, 0.76, and 1.08 V, respectively). As expected, the most Li-deficient phases, $LiAl_5O_8$, Li_2SiO_3, and $LiBO_2$, showed higher oxidation potentials.

Figure 5 shows the stability window for several promising ternary Na- and K-based coating materials. Figure 5a,c,b,d shows the most promising anode and cathode coatings. Compared to the Li compounds shown in Figure 3, many more compounds appear to be promising in the Na and K systems. For example, 35 Na and 46 K ternary compounds were identified as potential anode coatings (Figure 5a,c) compared to only 20 for Li (Figure 3a).

Regarding Na-based coatings, as shown in Figure 5a, three ternary fluorides, $NaYF_4$, Na_3ScF_6, and $NaMgF_3$, are predicted to have extremely wide stability windows of approximately 0−6 V. Two sulfides, $NaScS_2$ and $NaYS_2$ (window of 0−2.3 V), and three nitrides, $NaPN_2$, $NaSi_2N_3$, $NaGe_2N_3$ (window of 0−1.2 V), exhibited narrow windows but with good reductive stability. Oxides are the most common category of stable Na-based coatings for the interface between the anode and SE. A total of 27 Na ternary oxides were identified with reductive stabilities of at least 0.3 V. A full listing of the reduction and oxidation potentials of these compounds is presented in Table S4.

Figure 5b summarizes the promising Na-based coatings for use between the cathode and SE. A total of 17 fluorides, 6 chlorides, and 8 oxides were identified. In particular, $NaNO_3$, $Na_2B_8O_{13}$, $NaReO_4$, Na_2SeO_4, Na_2SO_4, $NaPO_3$, $NaBrO_3$, and $NaClO_4$ were identified as oxides with oxidative stabilities exceeding 4 V. Several other compositions were identified with slightly lower oxidation limits: $NaAlO_2$, Na_2SiO_3, $NaNbO_3$, $NaSbO_3$, and $NaGaO_2$ exhibited high oxidation potentials of 3.19, 3.15, 3.60, 3.99, and 3.24 V, respectively. The reduction and oxidation potential of all compounds shown in Figure 5b are listed in Table S5.

Regarding K-based systems, Figure 5c identifies 46 promising ternary coatings for the anode/SE interface. Five fluorides are predicted to have very wide stability windows ranging from 0 to 6 V. Likewise, $KCaCl_3$ exhibited a wide stability window of 0.3−4.6 V. A total of 36 K ternary oxides were also identified. Among these, $KAlO_2$, KBO_2, K_2MoO_4, $KNbO_3$, K_3PO_4, K_2SiO_3, and $KTaO_3$ also exhibited high oxidation potentials (ranging from 3.0 to 3.6 V) in addition to being stable against reduction. Regarding sulfides and nitrides, KYS_2, $KZrS_2$, $KCrN_2$, and $K_3P_6N_{11}$ were identified as stable coatings for use between the anode and SE. Table S6 lists the reduction and oxidation potentials of the K-based ternary compounds shown in Figure 5c.

Finally, Figure 5d shows that 21 fluorides, 3 chlorides, and 11 oxides were identified as K-based coating materials for use

DOI: 10.1021/acsami.9b11001
ACS Appl. Mater. Interfaces 2019, 11, 36607−36615

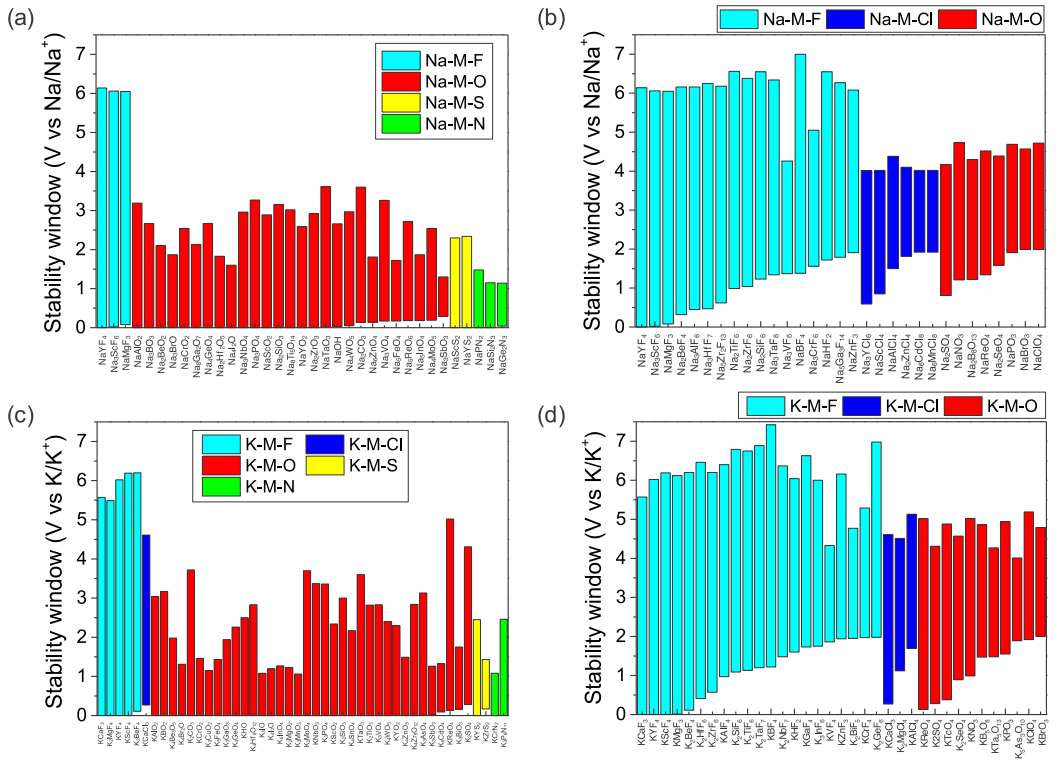

Figure 5. Stability window for (a,b) Na−M−X and (c,d) K−M−X ternary coating materials (X = F, Cl, O, S, and N) for use at (a,c) anode or (b,d) cathode.

Table 2. Lightweight, Transition-Metal-Free, and Potentially Low-Cost Coating Materials for Use in Li-, Na-, or K-Based Batteries at either the Anode/SE Interface (Left Columns, Favoring Stability at Low Potentials) or at the Cathode/SE Interface (Right Columns, Favoring Stability at High Potentials)[a]

for use at the anode/SE interface				for use at the cathode/SE interface			
	coating composition	reduction potential (V)	oxidation potential (V)		coating composition	reduction potential (V)	oxidation potential (V)
Li-based	Li_5AlO_4	0.06	3.04	Li-based	Li_3AlF_6	1.06	6.48
	$LiAlO_2$	0.17	3.7		$LiBF_4$	1.94	7.11
	Li_4SiO_4	0.26	3.41		$LiAlCl_4$	1.54	4.45
	Li_3BO_3	0.28	3.47		Li_3PO_4	0.69	4.21
	$LiSi_2N_3$	0.25	1.89		$LiAl_5O_8$	0.81	4.09
Na-based	$NaAlO_2$	0	3.19	Na-based	Na_3AlF_6	0.45	6.16
	Na_3BO_3	0	2.67		Na_2SiF_6	1.23	6.55
	Na_3PO_4	0	3.27		$NaBF_4$	1.38	7.00
	Na_2SiO_3	0	3.15		$NaAlCl_4$	1.50	4.38
	$NaSi_2N_3$	0	1.15		$NaPO_3$	1.91	4.69
K-based	$KAlO_2$	0	3.04	K-based	$KAlF_4$	0.97	6.4
	KBO_2	0	3.17		K_2SiF_6	1.09	6.79
	K_3PO_4	0	3.36		KBF_4	1.22	7.42
	K_2SiO_3	0	3.00		$KAlCl_4$	1.69	5.13
	$K_3P_6N_{11}$	0	2.46		KPO_3	1.55	4.94

[a]These materials are a subset of the coatings shown in Tables S2−S7.

between the cathode and SE. As with the Li- and Na-based systems, fluorides are generally the most stable against reduction. In addition, oxides such as KNO_3, $KReO_4$, K_2SO_4, K_2SeO_4, KPO_3, $KBrO_3$, and $KClO_4$ were identified as stable at slightly lower maximum voltages of 4 V. The reduction and oxidation potentials for the compounds in Figure 5d are listed in Table S7.

Thus far, our screening has targeted two classes of coatings: those that are stable against reduction (i.e., stable for voltages $\leq$ 0.3 V) and those that are stable against oxidation (i.e., stable for voltages $\geq$ 4 V). These criteria assume that thermodynamic equilibrium holds. Of course, slow kinetics can also inhibit the decomposition of a phase, even if that phase is predicted to decompose based on thermodynamic considerations. For example, because of slow mass transfer, a cathode coating predicted to be thermodynamically stable up to 4 V may not decompose if placed in contact with a cathode that operates at a slightly higher voltage.

DOI: 10.1021/acsami.9b11001
ACS Appl. Mater. Interfaces 2019, 11, 36607−36615

The possibility for "kinetic stabilization" leads us to also consider the coating materials that fall short of satisfying the strict stability criteria mentioned above. In this spirit, Table 1 shows the reduction and oxidation potentials for several Li-, Na-, and K-based oxides whose stability limits are not as aggressive as those reported above, but whose performance may be satisfactory in the presence of kinetic limitations. In particular, ternary oxides based on Ga, Nb, Sb, and Ta exhibit moderately high oxidation potentials ranging from 3.6 to 4.1 V in the case of Li-based oxides, 3.2−4.0 V for Na-based systems, and 3.1−3.8 V for K-based oxides. Additional ternary oxides based on Sn, Ge, Zr, Ti, Al, Si, and B oxides exhibit slightly lower oxidation potentials, Table 1.

On the basis of the materials predicted to exhibit promising electrochemical stability (and summarized in Tables S2−S7), Table 2 down-selects the coating compositions that are lightweight, transition-metal-free, and potentially low cost. The exclusion of transition-metal-based materials minimizes the possibility for undesirable electronic transport through the coating, which can occur through charge-hopping between redox-active transition metals. To our knowledge, all of the identified materials are "nonhypothetical" compounds that have been synthesized in prior experiments. Consistent with the broad trends identified in Figure 2d, coatings based on oxygen and nitrogen anions are the most prominent for anode/SE interfaces; for the cathode/SE interface, fluorides, chlorides, and oxides predominate.

It would be helpful to trace the stability trends across the different classes of materials shown in Figure 2d to fundamental properties of the materials themselves. One potential trend applies to the oxides and nitrides, which generally are the most stable against reduction (Figure 2d). On the basis of a screening study of ICSD, Sun et al.[42] reported that oxides and nitrides have on average the largest cohesive energies out of 11 types of inorganic solids. While this implies a link between reductive stability and cohesive energy, this relationship does not extend to the other categories of materials (fluorides, chlorides, sulfides, etc.). Beyond this weak correlation with cohesive energy, it is not obvious which other properties might explain electrochemical stability. Earlier work[43] suggests that the stability can depend on the band edge positions of the coating/SE relative to the electrochemical potential of the relevant electrode. However, calculating these positions accurately is computationally expensive and thus impractical for the many materials screened here. In sum, a thorough analysis of stability trends will likely require significant effort and is therefore best left to a stand-alone publication.

CONCLUSIONS

The development of SEs has the potential to enhance the energy density and safety of rechargeable batteries. One challenge to attaining this goal, however, is reactivity between the SE and the electrodes: these reactions can form new interphases with high resistivity. A potential solution to this challenge is to employ thin coatings between the electrolyte and electrodes. In principle, the use of a thin, stable coating can prevent (or limit the extent of) these undesirable reactions.

Toward the goal of identifying appropriate coatings, the present study has assessed more than 1300 binary and ternary materials for use in all solid-state Li, Na, and K batteries. The stability windows of these candidate coating materials was examined as a function of potential (V) relative to Li/Li^+, Na/Na^+, or K/K^+ using the grand potential phase diagram method implemented in the Materials Project. The coating compositions considered include fluorides, chlorides, oxides, sulfides, phosphides, and nitrides.

In the case of binary compounds, the halides and chalcogenides exhibited the best stability when in contact with a metal anode. Binary fluorides exhibit wide stability windows, highlighting their suitability for use as coating materials at the SE/cathode interface. For the ternary compounds, the fluorides and chlorides exhibit the highest oxidative stabilities, suggesting that they are appropriate choices for stabilizing SE/cathode interfaces. In contrast, sulfides, phosphides, and nitrides exhibit much lower oxidative stabilities, with many of these materials predicted to decompose above 2 V. At the anode/SE interface, nitrides and oxides are predicted to be the most effective coatings, as they are generally the most stable against reductive decomposition. As expected, the sulfides and phosphides are the least stable class of materials under reducing conditions. Overall, the oxides appear to be the most versatile class of coating materials: several oxides are predicted to exhibit stability windows ranging from 0 to 3 V with respect to Li/Li^+, Na/Na^+, or K/K^+. Examples of promising oxides for stabilizing the SE/anode interface include Li_5AlO_4, Li_4SiO_4, $NaAlO_2$, Na_3PO_4, $KAlO_2$, and K_3PO_4. Similarly, promising compounds for stabilizing the SE/cathode interface include $NaPO_3$ and KPO_3. Finally, the possibility for kinetic stabilization suggests that additional ternary oxides (based, e.g., on Ga, Nb, Sb, and Ta) may be viable coatings at the SE/cathode interface despite the fact that these materials have slightly lower oxidative stabilities.

ASSOCIATED CONTENT

Supporting Information

The Supporting Information is available free of charge on the ACS Publications website at DOI: 10.1021/acsami.9b11001.

Reduction and oxidation potential of Li, Na, and K coating materials (PDF)

AUTHOR INFORMATION

Corresponding Authors

*E-mail: shyu@kist.re.kr. Phone: +82-2-958-5232 (S.Y.).
*E-mail: djsiege@umich.edu. Phone: +1 (734) 764-4808 (D.J.S.).

ORCID

Seungho Yu: 0000-0003-3912-6463
Haesun Park: 0000-0001-6266-8151
Donald J. Siegel: 0000-0001-7913-2513

Notes

The authors declare no competing financial interest.

ACKNOWLEDGMENTS

The authors acknowledge the financial support from the U.S. Department of Energy, Advanced Research Projects Agency—Energy, grant no. DE-AR0000653. This research was partly supported by the Technology Development Program to Solve Climate Changes of the National Research Foundation (NRF) funded by the Ministry of Science & ICT of Korea (2017M1A2A204482) and by the institutional program of the Korea Institute of Science and Technology (project nos.

DOI: 10.1021/acsami.9b11001
ACS Appl. Mater. Interfaces 2019, 11, 36607−36615

2E29642 and 2E29900). D.J.S and S.Y. thank N. Dasgupta and J. Sakamoto for helpful discussions.

REFERENCES

(1) Bruce, P. G.; Freunberger, S. A.; Hardwick, L. J.; Tarascon, J.-M. Li−O_2 and Li−S batteries with high energy storage. *Nat. Mater.* **2012**, *11*, 19.

(2) Larcher, D.; Tarascon, J.-M. Towards Greener and More Sustainable Batteries for Electrical Energy Storage. *Nat. Chem.* **2015**, *7*, 19.

(3) Li, J.; Ma, C.; Chi, M.; Liang, C.; Dudney, N. J. Solid Electrolyte: the Key for High-Voltage Lithium Batteries. *Adv. Energy Mater.* **2015**, *5*, 1401408.

(4) Yang, C.; Fu, K.; Zhang, Y.; Hitz, E.; Hu, L. Protected Lithium-Metal Anodes in Batteries: From Liquid to Solid. *Adv. Mater.* **2017**, *29*, 1701169.

(5) Liu, Y.; He, P.; Zhou, H. Rechargeable Solid-State Li−Air and Li−S Batteries: Materials, Construction, and Challenges. *Adv. Energy Mater.* **2018**, *8*, 1701602.

(6) Lin, D.; Liu, Y.; Cui, Y. Reviving the Lithium Metal Anode for High-Energy Batteries. *Nat. Nanotechnol.* **2017**, *12*, 194.

(7) Goodenough, J. B.; Kim, Y. Challenges for Rechargeable Li Batteries. *Chem. Mater.* **2010**, *22*, 587−603.

(8) Bachman, J. C.; Muy, S.; Grimaud, A.; Chang, H.-H.; Pour, N.; Lux, S. F.; Paschos, O.; Maglia, F.; Lupart, S.; Lamp, P.; Giordano, L.; Shao-Horn, Y. Inorganic Solid-State Electrolytes for Lithium Batteries: Mechanisms and Properties Governing Ion Conduction. *Chem. Rev.* **2016**, *116*, 140−162.

(9) Yamauchi, A.; Sakuda, A.; Hayashi, A.; Tatsumisago, M. Preparation and ionic conductivities of $(100 - x)(0.75Li_2S \cdot 0.25P_2S_5) \cdot xLiBH_4$ glass electrolytes. *J. Power Sources* **2013**, *244*, 707−710.

(10) Murugan, R.; Thangadurai, V.; Weppner, W. Fast Lithium Ion Conduction in Garnet-Type $Li_7La_3Zr_2O_{12}$. *Angew. Chem., Int. Ed.* **2007**, *46*, 7778−7781.

(11) Kanno, R.; Hata, T.; Kawamoto, Y.; Irie, M. Synthesis of a New Lithium Ionic Conductor, Thio-LISICON−Lithium Germanium Sulfide System. *Solid State Ionics* **2000**, *130*, 97−104.

(12) Kato, Y.; Hori, S.; Saito, T.; Suzuki, K.; Hirayama, M.; Mitsui, A.; Yonemura, M.; Iba, H.; Kanno, R. High-Power All-Solid-State Batteries Using Sulfide Superionic Conductors. *Nat. Energy* **2016**, *1*, 16030.

(13) Kamaya, N.; Homma, K.; Yamakawa, Y.; Hirayama, M.; Kanno, R.; Yonemura, M.; Kamiyama, T.; Kato, Y.; Hama, S.; Kawamoto, K.; Mitsui, A. A Lithium Superionic Conductor. *Nat. Mater.* **2011**, *10*, 682.

(14) Koerver, R.; Aygün, I.; Leichtweiß, T.; Dietrich, C.; Zhang, W.; Binder, J. O.; Hartmann, P.; Zeier, W. G.; Janek, J. Capacity Fade in Solid-State Batteries: Interphase Formation and Chemomechanical Processes in Nickel-Rich Layered Oxide Cathodes and Lithium Thiophosphate Solid Electrolytes. *Chem. Mater.* **2017**, *29*, 5574−5582.

(15) Zhu, Y.; He, X.; Mo, Y. Origin of Outstanding Stability in the Lithium Solid Electrolyte Materials: Insights from Thermodynamic Analyses Based on First-Principles Calculations. *ACS Appl. Mater. Interfaces* **2015**, *7*, 23685−23693.

(16) Zhu, Y.; He, X.; Mo, Y. First principles study on electrochemical and chemical stability of solid electrolyte−electrode interfaces in all-solid-state Li-ion batteries. *J. Mater. Chem. A* **2016**, *4*, 3253−3266.

(17) Richards, W. D.; Miara, L. J.; Wang, Y.; Kim, J. C.; Ceder, G. Interface Stability in Solid-State Batteries. *Chem. Mater.* **2016**, *28*, 266−273.

(18) Chu, I.-H.; Nguyen, H.; Hy, S.; Lin, Y.-C.; Wang, Z.; Xu, Z.; Deng, Z.; Meng, Y. S.; Ong, S. P. Insights into the Performance Limits of the $Li_7P_3S_{11}$ Superionic Conductor: A Combined First-Principles and Experimental Study. *ACS Appl. Mater. Interfaces* **2016**, *8*, 7843−7853.

(19) Lacivita, V.; Wang, Y.; Bo, S.-H.; Ceder, G. Ab Initio Investigation of the Stability of Electrolyte/Electrode Interfaces in All-Solid-State Na Batteries. *J. Mater. Chem. A* **2019**, *7*, 8144−8155.

(20) Tang, H.; Deng, Z.; Lin, Z.; Wang, Z.; Chu, I.-H.; Chen, C.; Zhu, Z.; Zheng, C.; Ong, S. P. Probing Solid-Solid Interfacial Reactions in All-Solid-State Sodium-Ion Batteries with First-Principles Calculations. *Chem. Mater.* **2018**, *30*, 163−173.

(21) Han, X.; Gong, Y.; Fu, K.; He, X.; Hitz, G. T.; Dai, J.; Pearse, A.; Liu, B.; Wang, H.; Rubloff, G.; Mo, Y.; Thangadurai, V.; Wachsman, E. D.; Hu, L. Negating Interfacial Impedance in Garnet-Based Solid-State Li Metal Batteries. *Nat. Mater.* **2016**, *16*, 572.

(22) Song, Y.; Yang, L.; Zhao, W.; Wang, Z.; Zhao, Y.; Wang, Z.; Zhao, Q.; Liu, H.; Pan, F. Revealing the Short-Circuiting Mechanism of Garnet-Based Solid-State Electrolyte. *Adv. Energy Mater.* **2019**, *9*, 1900671.

(23) Jung, S. H.; Oh, K.; Nam, Y. J.; Oh, D. Y.; Brüner, P.; Kang, K.; Jung, Y. S. Li_3BO_3−Li_2CO_3: Rationally Designed Buffering Phase for Sulfide All-Solid-State Li-Ion Batteries. *Chem. Mater.* **2018**, *30*, 8190−8200.

(24) Sakuda, A.; Hayashi, A.; Tatsumisago, M. Interfacial Observation between $LiCoO_2$ Electrode and Li_2S−P_2S_5 Solid Electrolytes of All-Solid-State Lithium Secondary Batteries Using Transmission Electron Microscopy. *Chem. Mater.* **2010**, *22*, 949−956.

(25) Takahashi, K.; Hattori, K.; Yamazaki, T.; Takada, K.; Matsuo, M.; Orimo, S.; Maekawa, H.; Takamura, H. All-solid-state lithium battery with $LiBH_4$ solid electrolyte. *J. Power Sources* **2013**, *226*, 61−64.

(26) Xiao, Y.; Miara, L. J.; Wang, Y.; Ceder, G. Computational Screening of Cathode Coatings for Solid-State Batteries. *Joule* **2019**, *3*, 1252−1275.

(27) Pfenninger, R.; Struzik, M.; Garbayo, I.; Stilp, E.; Rupp, J. L. M. A Low Ride on Processing Temperature for Fast Lithium Conduction in Garnet Solid-State Battery Films. *Nat. Energy* **2019**, *4*, 475−483.

(28) Wang, C.; Gong, Y.; Liu, B.; Fu, K.; Yao, Y.; Hitz, E.; Li, Y.; Dai, J.; Xu, S.; Luo, W.; Wachsman, E. D.; Hu, L. Conformal, Nanoscale ZnO Surface Modification of Garnet-Based Solid-State Electrolyte for Lithium Metal Anodes. *Nano Lett.* **2017**, *17*, 565−571.

(29) Albertus, P.; Babinec, S.; Litzelman, S.; Newman, A. Status and Challenges in Enabling the Lithium Metal Electrode for High-Energy and Low-Cost Rechargeable Batteries. *Nat. Energy* **2018**, *3*, 16−21.

(30) Jain, A.; Hautier, G.; Moore, C. J.; Ping Ong, S.; Fischer, C. C.; Mueller, T.; Persson, K. A.; Ceder, G. A High-Throughput Infrastructure for Density Functional Theory Calculations. *Comput. Mater. Sci.* **2011**, *50*, 2295−2310.

(31) Blöchl, P. E. Projector Augmented-Wave Method. *Phys. Rev. B: Condens. Matter Mater. Phys.* **1994**, *50*, 17953−17979.

(32) Perdew, J. P.; Burke, K.; Ernzerhof, M. Generalized Gradient Approximation Made Simple. *Phys. Rev. Lett.* **1996**, *77*, 3865−3868.

(33) Kresse, G.; Furthmüller, J. Efficient iterative schemes forab initiototal-energy calculations using a plane-wave basis set. *Phys. Rev. B: Condens. Matter Mater. Phys.* **1996**, *54*, 11169−11186.

(34) Ong, S. P.; Richards, W. D.; Jain, A.; Hautier, G.; Kocher, M.; Cholia, S.; Gunter, D.; Chevrier, V. L.; Persson, K. A.; Ceder, G. Python Materials Genomics (Pymatgen): A Robust, Open-Source Python Library for Materials Analysis. *Comput. Mater. Sci.* **2013**, *68*, 314−319.

(35) Wang, L.; Maxisch, T.; Ceder, G. Oxidation energies of transition metal oxides within the GGA + *U* framework. *Phys. Rev. B: Condens. Matter Mater. Phys.* **2006**, *73*, 195107.

(36) Jain, A.; Hautier, G.; Ong, S. P.; Moore, C. J.; Fischer, C. C.; Persson, K. A.; Ceder, G. Formation Enthalpies by Mixing GGA and GGA + *U* Calculations. *Phys. Rev. B: Condens. Matter Mater. Phys.* **2011**, *84*, 045115.

(37) Ong, S. P.; Wang, L.; Kang, B.; Ceder, G. Li−Fe−P−O_2 Phase Diagram from First Principles Calculations. *Chem. Mater.* **2008**, *20*, 1798−1807.

(38) Schmidt, J.; Shi, J.; Borlido, P.; Chen, L.; Botti, S.; Marques, M. A. L. Predicting the Thermodynamic Stability of Solids Combining

DOI: 10.1021/acsami.9b11001
ACS Appl. Mater. Interfaces 2019, 11, 36607−36615

Density Functional Theory and Machine Learning. *Chem. Mater.* **2017**, *29*, 5090−5103.
(39) Kazyak, E.; Chen, K.-H.; Davis, A. L.; Yu, S.; Sanchez, A. J.; Lasso, J.; Bielinski, A. R.; Thompson, T.; Sakamoto, J.; Siegel, D. J.; Dasgupta, N. P. Atomic Layer Deposition and First Principles Modeling of Glassy Li_3BO_3−Li_2CO_3 Electrolytes for Solid-State Li Metal Batteries. *J. Mater. Chem. A* **2018**, *6*, 19425−19437.
(40) Schnell, J.; Tietz, F.; Singer, C.; Hofer, A.; Billot, N.; Reinhart, G. Prospects of Production Technologies and Manufacturing Costs of Oxide-Based All-Solid-State Lithium Batteries. *Energy Environ. Sci.* **2019**, *12*, 1818−1833.
(41) Zhu, Y.; He, X.; Mo, Y. Strategies Based on Nitride Materials Chemistry to Stabilize Li Metal Anode. *Adv. Sci.* **2017**, *4*, 1600517.
(42) Sun, W.; Dacek, S. T.; Ong, S. P.; Hautier, G.; Jain, A.; Richards, W. D.; Gamst, A. C.; Persson, K. A.; Ceder, G. The Thermodynamic Scale of Inorganic Crystalline Metastability. *Sci. Adv.* **2016**, *2*, No. e1600225.
(43) Thompson, T.; Yu, S.; Williams, L.; Schmidt, R. D.; Garcia-Mendez, R.; Wolfenstine, J.; Allen, J. L.; Kioupakis, E.; Siegel, D. J.; Sakamoto, J. Electrochemical Window of the Li-Ion Solid Electrolyte $Li_7La_3Zr_2O_{12}$. *ACS Energy Lett.* **2017**, *2*, 462−468.

DOI: 10.1021/acsami.9b11001
ACS Appl. Mater. Interfaces 2019, 11, 36607−36615